NUMERICAL COMPUTATION OF EXHAUST NOISE THROUGH PERFORATED DIFFUSER USING OPTIMIZED HIGH-ORDER COMPACT SCHEMES

Jae Wook Kim and Duck Joo Lee

Korea Advanced Institute of Science and Technology
Department of Aerospace Engineering, 373-1 Kusong-dong, Yusong-gu, Taejon, KOREA

ABSTRACT

Exhaust noise from an electrical power plant is generated owing to high pressure inside the boiler when the gas is suddenly exhausted through a safety valve. To reduce the noise, an expansion chamber with a perforated diffuser is used. Noise generation, propagation and radiation from the exhaust gas system are numerically simulated to investigate the noise generation mechanism and to design the efficient perforated diffuser. The high-order compact schemes which were optimized in the wavenumber domain for high-resolution characteristics are used in this numerical simulation. The OHOC schemes are non-dissipative and much less dispersive than the other low-order standard schemes, and well adapted to computational aeroacoustic (CAA) problems. The OHOC schemes are coupled with the artificial dissipation terms and the fourth-order low dissipation and dispersion Runge-Kutta (LDDRK) time-marching method for solving nonlinear unsteady Euler equations accurately. The characteristics-based boundary conditions are implemented as physical boundary conditions for the OHOC schemes. It is shown that the application of these schemes to simulation of the exhaust gas noise reduction system presents time accurate results with partially oscillating supersonic flows near the perforated diffuser and the reduced acoustic pressure fields through the expansion chamber.

I. INTRODUCTION

The optimized high-order compact (OHOC) schemes proposed by Kim and Lee [1-3] are properly formulated to achieve maximum spatial resolution that they are less dissipative and dispersive than the other low-order standard schemes. It has been generally recognized that the high-order low dispersion and dissipation schemes are less suitable for the computation of nonlinear wave solutions with high discontinuity. It was found that the nonlinear wave steepening process, when viewed in the wavenumber domain, corresponded to an energy cascade process whereby low wavenumber components are transferred to high wavenumber range [4]. When shocks are formed, it is known these schemes generally produce spurious spatial oscillations around them and in regions with steep gradients. These spurious oscillations are waves from the unresolved high wavenumber range generated by the nonlinear wave cascading process. Currently, there are many well-established shock-capturing schemes in the

literature [5-10]. Most shock-capturing schemes are generally low-order upwind ones with substantial built-in artificial dissipation, and they are not designed or suitable for computations of long distance wave propagation. The OHOC schemes are so low dissipative; that is, they have no built-in artificial dissipation. To be applicable to the nonlinear wave problems, they require an effective artificial dissipation algorithm to damp out the spurious oscillations [11,12].

An efficient high-order low dissipation and dispersion time advancing method is needed to produce time-accurate solutions of long distance linear or nonlinear wave propagation with correct wave speeds and profiles. The OHOC schemes in space are low dispersive and dissipative to provide high-resolution characteristics, thus it is recommended to use such a time advancing method for space-time consistency. The Runge-Kutta schemes were optimized to achieve minimized dissipation and dispersion errors for the propagating waves, rather than to obtain the maximum formal order of accuracy and these are referred to as low dissipation and dispersion Runge-Kutta (LDDRK) method [14]. The fourth-order LDDRK scheme with two steps of four-six alternating stages is so efficient that it can use two times larger time step spacing than the classical fourth-order Runge-Kutta scheme within an accuracy limit.

Correct and physical boundary conditions should be imposed to yield high-quality wave solutions. Recently, several suggestions for the physical boundary conditions have been proposed for the unsteady aeroacoustic computations. These proposals can be classified in three categories, i.e., (1) quasi one-dimensional characteristics, (2) decomposition of the solution into Fourier modes, and (3) asymptotic analysis of the governing equations for large distances [13,15-17]. The high-order compact schemes are sensitive to boundary values in the evaluation of the first derivatives, so the quality of solutions even on the interior nodes depend on the accuracy of the boundary conditions. In this reason, the correct and physical boundary conditions are important for the actual applications of the OHOC schemes.

The conservative forms of Euler equations are solved by these numerical algorithms. The whole flow and acoustic fields produced by high pressure and temperature gas flow in and out of a perforated diffuser with an expansion chamber are simulated in axisymmetric coordinates. Gas noise induced by vibration of strong shocks and instability of inviscid supersonic jets near perforated diffuser is computed in far field region located in the expansion chamber. It seems that the numerical analysis of the gas noise sources near the perforated diffuser and the resulting far-field noise can guide to a better noise reduction method and a solution of industrial gas noise problem.

II. GOVERNING EQUATIONS

The linear and nonlinear waves are computed from the Euler equations. The conservative forms of one-, two-dimensional and axisymmetric Euler equations in the Cartesian coordinates are considered in this paper.

$$\frac{\partial Q}{\partial t} + \frac{\partial E}{\partial x} + \frac{\partial F}{\partial y} + \alpha H = 0 \tag{2.1}$$

where

$$Q = \begin{bmatrix} \rho \\ \rho u \\ \rho v \\ \rho e_t \end{bmatrix}, \quad E = \begin{bmatrix} \rho u \\ \rho u^2 + p \\ \rho u v \\ (\rho e_t + p) u \end{bmatrix}, \quad F = \begin{bmatrix} \rho v \\ \rho v u \\ \rho v^2 + p \\ (\rho e_t + p) v \end{bmatrix} \quad \text{and} \quad H = \frac{1}{y} \begin{bmatrix} \rho v \\ \rho u v \\ \rho v^2 \\ (\rho e_t + p) v \end{bmatrix}$$

The axisymmetric and two-dimensional equations are formulated in cases of $\alpha = 1$ and $\alpha = 0$ respectively. The spatial derivative terms in Eq. (2.1) are evaluated by the OHOC schemes. For the nonlinear wave computations, the artificial dissipation terms[2,11,12] can be added in the right hand side of Eq. (2.1) as a treatment of the nonlinearity. Time advancing method is the fourth-order low dissipation and dispersion Runge-Kutta (LDDRK) scheme that has two steps of four-six alternating stages [3,14].

III. NUMERICAL ALGORITHMS

III-1. OHOC Schemes on Interior Nodes

The main schemes presented here are generalizations of Pade' scheme of seven-point stencil as shown below [1,19] :

$$\beta f'_{i-2} + \alpha f'_{i-1} + f'_i + \alpha f'_{i+1} + \beta f'_{i+2} = a\frac{f_{i+1}-f_{i-1}}{2\Delta x} + b\frac{f_{i+2}-f_{i-2}}{4\Delta x} + c\frac{f_{i+3}-f_{i-3}}{6\Delta x} \qquad (3.1)$$

This is the central difference formulation for computations on interior nodes. Only the eighth-order tridiagonal ($\beta = 0$) scheme and the tenth-order pentadiagonal ($\beta \neq 0$) scheme have unique values of the coefficients a,b,c,α and β, and these are the highest-order ones. The other lower-order schemes should have free coefficients that are not determined completely until more constraints are imposed and these would be able to improve the resolution characteristics. The analytic and systematic constraints for determination of the free coefficients are considered. The nature of these constraints is to minimize the dispersive (phase) errors in the wavenumber domain by using Fourier analysis. Kim and Lee [1] proposed the analytic optimization methods to achieve the OHOC schemes and showed that the optimized sixth-order tridiagonal (OSOT) and fourth-order pentadiagonal (OFOP) scheme are more effective than that of any other compact scheme. The coefficients of the OSOT and OFOP scheme are presented in Ref. 1 and these provide the high-order accuracy and the maximum resolution for the central compact schemes. The maximum resolution characteristics of the OHOC schemes are compared with those of other standard central schemes in Fig. 1.
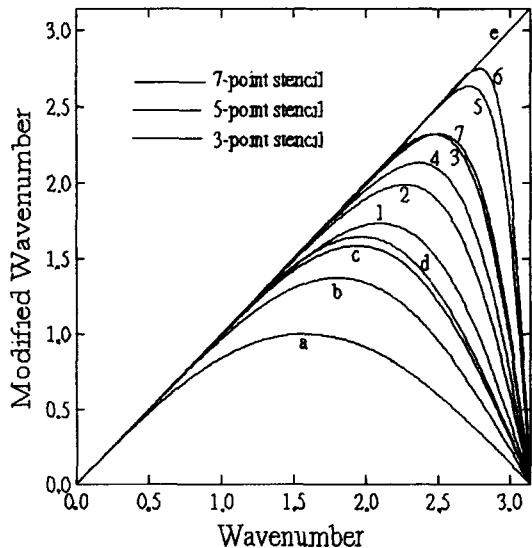

Fig. 1 Maximum resolution characteristics of the OHOC schemes in comparison with the other standard schemes
a : second-order central differences
b : fourth-order central differences
c : sixth-order central differences
d : Tam's DRP scheme in space
e : exact differentiation
1 : standard Pade' scheme
2 : sixth-order tridiagonal scheme ($c = 0$)
3 : OSOT (optimized sixth-order tridiagonal) scheme
4 : eighth-order tridiagonal scheme
5 : Lele's fourth-order spectral-like pentadiagonal scheme
6 : OFOP (optimized fourth-order pentadiagonal) scheme
7 : tenth-order pentadiagonal scheme

III-2. OHOC Schemes on Near-Boundary Nodes

The optimized near-boundary compact schemes are considered for accurate computations in domain with non-periodic boundaries. The schemes on interior nodes use seven-point stencil, thus three kinds of near-boundary schemes are required on three nodes ($i = 0$, 1 and 2) from the boundary ($i = 0$). The near-boundary compact differences are formulated as follows [3,19] :

$$i = 0 \ : \quad f_0' + \alpha_{0,1} f_1' + \beta_{0,2} f_2' = \frac{1}{\Delta x} \sum_{j=0}^{3} a_{0,j} f_j \tag{3.2}$$

$$i = 1 \ : \quad \alpha_{1,0} f_0' + f_1' + \alpha_{1,2} f_2' + \beta_{1,3} f_3' = \frac{1}{\Delta x} \sum_{j=0}^{4} a_{1,j} f_j \tag{3.3}$$

$$i = 2 \ : \quad \beta_{2,0} f_0' + \alpha_{2,1} f_1' + f_2' + \alpha_{2,3} f_3' + \beta_{2,4} f_4' = \frac{1}{\Delta x} \sum_{j=0}^{5} a_{2,j} f_j \tag{3.4}$$

where, all the β_j's should be equal to zero for the tridiagonal schemes. These formulations are, of necessity, non-central differences and their error characteristics are both dispersive and dissipative. The two kinds of errors can be analyzed simultaneously in the wavenumber domain by the Fourier analysis. The dispersive and the dissipative errors of the near-boundary compact schemes were minimized by the analytic optimization methods proposed by Kim and Lee [3]. The coefficients α_j's, β_j's and a_j's of the optimized near-boundary compact schemes are presented in Ref. 3 and these provide the high accuracy and the maximum resolution for the near-boundary compact schemes. The maximum resolution characteristics of the optimized near-boundary compact schemes are presented in Fig. 2.
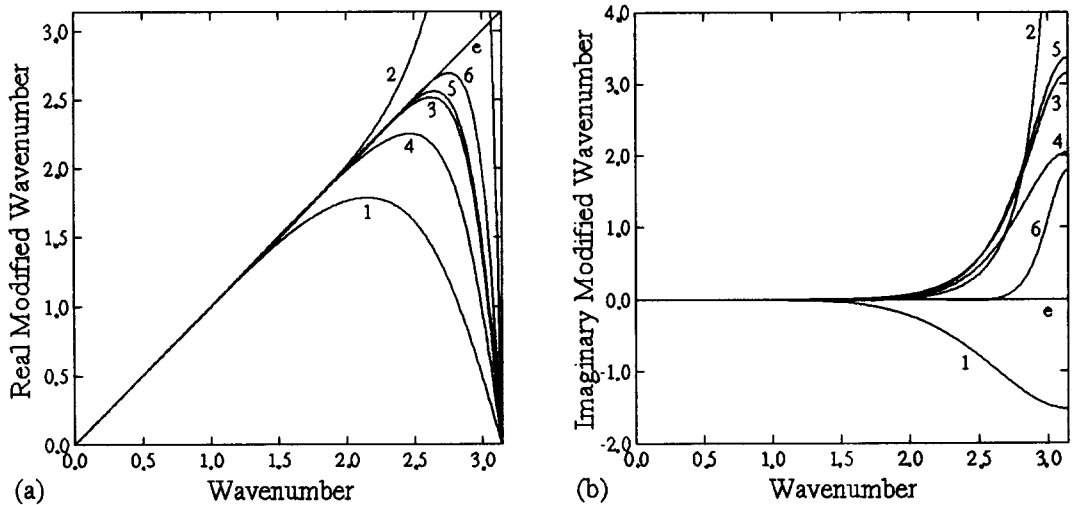

Fig. 2 Maximum resolution characteristics of the optimized near-boundary compact schemes
(a) dispersive characteristics   (b) dissipative characteristics
1 : second-order tridiagonal scheme for $i = 0$ 4 : second-order pentadiagonal scheme for $i = 0$
2 : fourth-order tridiagonal scheme for $i = 1$ 5 : fourth-order pentadiagonal scheme for $i = 1$
3 : sixth-order tridiagonal scheme for $i = 2$ 6 : fourth-order pentadiagonal scheme for $i = 2$

III-3. Treatment of Nonlinearity

The problem considered here includes nonlinear waves with discontinuities. Such nonlinear

waves can cause serious numerical instabilities and errors that result in spurious numerical oscillations when the numerical algorithms are not suited to the nonlinearity. Therefore it is necessary to eliminate the spurious numerical wave components in the narrow band of high wavenumber range, while at the same time keeping the wave components in the wide band of low wavenumber range unaffected. This can be achieved by inserting artificial dissipation terms in the finite difference equations [11,12]. They can be easily combined with the OHOC schemes explicitly. The artificial dissipation terms are used as a treatment of nonlinearity for the OHOC schemes in this paper.

III-4. Low Dissipation and Dispersion Time Advancing

The OHOC schemes are non-dissipative and low dispersive to provide high-resolution characteristics in space for a given stencil. Thus, the time advancing method for them should be also an efficient high-order less dissipation and dispersion scheme than the other standard ones. The Runge-Kutta method were optimized to be a low dissipation and dispersion time advancing method for various truncation orders in Ref. [14] and it is referred as LDDRK method. The fourth-order LDDRK method which is used in this paper for the OHOC schemes includes two steps of four-six alternating stages and it is more efficient than the classical fourth-order Runge-Kutta method with four stages. When two steps are combined in the optimization, the dissipation and dispersion errors can be further reduced and the high-order accuracy can be maintained.

III-5. Physical Boundary Conditions

For the present work, Thompson's characteristics-based boundary conditions are used as the physical boundary conditions for the multi-dimensional computation [16]. He decomposed the Euler equations into wave modes of definite velocity and then specified boundary conditions for the incoming waves. The amplitudes of the outward propagating waves are defined entirely from the variables inside the computational domain, while those of the inward propagating waves are specified as the boundary conditions. One important drawback in the characteristics-based boundary conditions is that there are no true characteristics in two- or three-dimensional problems. As an approximation, one may ignore the multi-dimensionality of a problem at a boundary, and treat the problem as if the problem is locally one-dimensional with the direction normal to the boundary. For the radiation or outflow boundary conditions, this approximation has been found to lead to significant non-physical reflections when the incident angles of waves are oblique to the boundary and also when there is a strong mean flow tangent to the boundary [20].

IV. NUMERICAL COMPUTATIONS

In this paper, the flow and acoustic fields produced by high pressure and temperature gas flow in and out of a perforated diffuser with an expansion chamber are simulated numerically. The conservative forms of Euler equations in axisymmetric coordinates are solved with initial conditions imposed in the inlet region of the diffuser. The initial inlet and ambient value are imposed in the ratio of 1.44:1 for pressure, 1.65:1 for density and the Mach number of the inlet flow is 1.0. Steam is considered as the gas and its specific heat ratio is 1.3. These initial conditions come out when a safety valve of steam boiler used for electrical power plant is open and the steam flow arrives at the inlet region of diffuser silencer. The safety valve get open only

if pressure inside the boiler is greater than 100 times of ambient pressure, so the steam flow through the perforated diffuser and expansion chamber is of high pressure, temperature and speed.

Grid system for the present computations is shown in Fig. 3. Many grids are clustered inside the diffuser and near the holes where large fluctuation of flow exists. There are three hole strips around the diffuser and total area of the hole strips and cross section area of the inlet pipe are in the ratio of 2.85:1. A snap shot of pressure field (pressure contours) is presented in Fig. 4 as a result of computations. It is shown that there are oscillating shocks inside the diffuser and shedding vortices through the hole strips due to supersonic jets, which result in the major noise sources in this system. Far-field acoustic signals are obtained at four locations outside the expansion chamber as pointed by alphabet a, b, c and d in Fig. 3. Plots of the obtained acoustic signals and the measured noise levels are presented in Fig. 5.
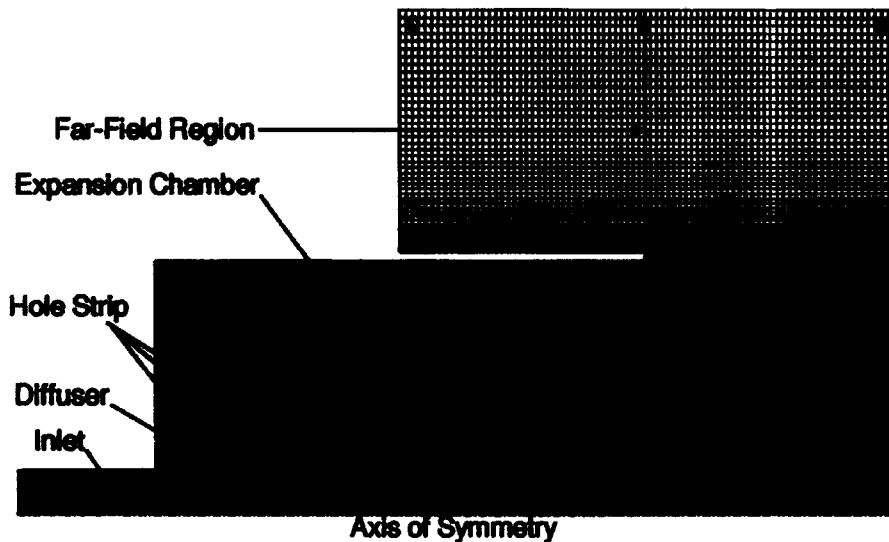

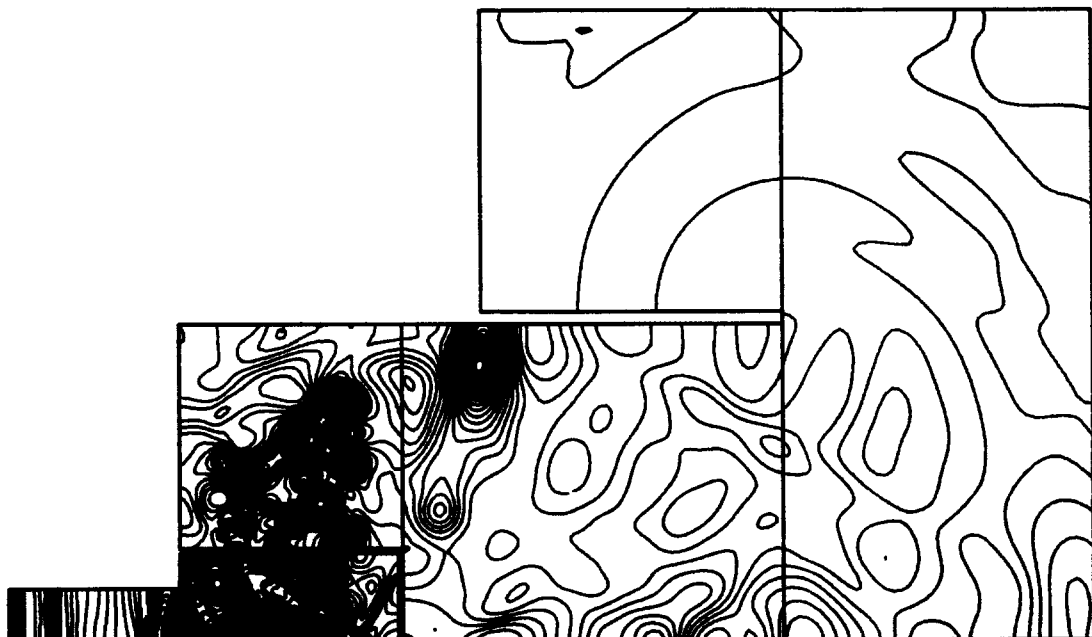**Fig. 3** Grid system of perforated diffuser and expansion chamber for numerical computation

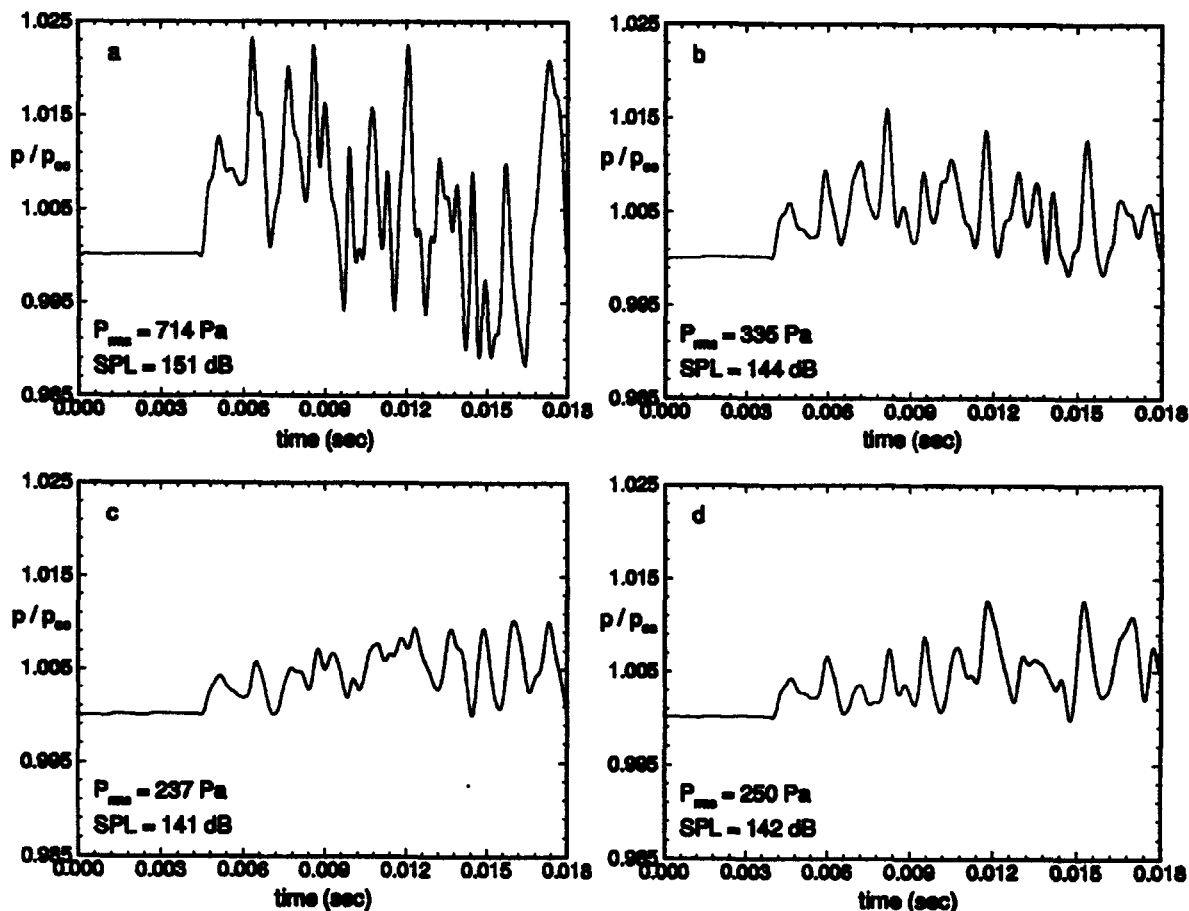**Fig. 4** Pressure field induced by steam gas flow through perforated diffuser

Fig. 5 Far-field noise signal and measured noise level

REFERENCES

[1] Kim, J. W., and Lee, D. J., "Optimized Compact Finite Difference Schemes with Maximum Resolution," *AIAA Journal*, Vol. 34, No. 5, 1996, pp. 887-893.

[2] Kim, J. W., and Lee, D. J., "Numerical Simulation of Nonlinear Waves Using Optimized High-Order Compact Schemes," *CFD Journal*, Vol. 5, No. 3, 1996, pp. 281-300.

[3] Kim, J. W., and Lee, D. J., "Implementation of Boundary Conditions for the Optimized High-Order Compact Schemes," *Journal of Computational Acoustics*, Vol. 5, No. 2, 1997, pp. 177-191.

[4] Tam, C. K. W., "Computational Aeroacoustics : Issues and Methods," AIAA Paper 95-0677, January 1995.

[5] Roe, P. L. , " Characteristic-Based Schemes for the Euler Equations," *Annual Review of Fluid Mechanics*, Vol. 18, 1986, pp. 337-365.

[6] Yee, H. C., Warming, R. F., and Harten, A., "Implicit Total-Variation-Diminishing (TVD) Schemes for Steady State Calculations," *Journal of Computational Physics*, Vol. 57, 1985, pp. 327-360.

[7] Harten, A., and Osher, S., "Nonuniformly High-Order Accurate Nonoscillatory Schemes," *SIAM Journal of Numerical Analysis*, Vol. 24, 1987, pp. 279-309.

[8] Van Leer, B., "Towards the Ultimate Conservative Difference Scheme, V. A Second-Order Sequel to Godunov's Method," *Journal of Computational Physics*, Vol. 32, 1979, pp. 101-136.

[9] Colella, P., and Woodward, P. R., "The Piecewise Parabolic Method (PPM) for Gasdynamical Simulations," *Journal of Computational Physics*, Vol. 54, 1984, pp. 174-201.

[10] Yang, H. Q., and Przekwas, A. J., "A Comparative Study of Advanced Shock-Capturing Schemes Applied to Burger's Equation," *Journal of Computational Physics*, Vol. 102, 1992, pp. 139-159.

[11] Jameson, A., Schmidt, W., and Turkel, E., "Numerical Simulation of the Euler equations by Finite Volume Methods Using Runge-Kutta Time Stepping Schemes," AIAA Paper 81-1259, 1981.

[12] Pulliam, T. H., "Artificial Dissipation Models for the Euler Equations," AIAA Paper 85-0438, 1985.

[13] Tam, C. K. W., and Webb, J. C., "Dispersion-Relation-Preserving Finite Difference Schemes for Computational Acoustics," *Journal of Computational Physics*, Vol. 107, 1993, pp. 262-281.

[14] Hu, F. Q., Hussaini, M. Y., and Manthey, J., "Application of Low Dissipation and Low Dispersion Runge-Kutta Schemes to Benchmark Problems in Computational Aeroacoustics," *Proceedings of ICASE/LaRC Workshop on Benchmark Problems in Computational Aeroacoustics*, U.S.A., October 1994, pp. 73-98.

[15] Hixon, R., Shih, S. H., and Mankbadi, R. R., "Evaluation of Boundary Conditions for Computational Aeroacoustics," AIAA Paper 95-0160, January 1995.

[16] Thompson, K. W., "Time-Dependent Boundary Conditions for Hyperbolic Systems, II," *Journal of Computational Physics*, Vol. 89, 1990, pp. 439-461.

[17] Giles, M. B., "Nonreflecting Boundary Conditions for Euler Equation Calculations," *AIAA Journal*, Vol. 28, No. 12, 1990, pp. 2050-2058.

[18] Lee, D. J., and Koo, S. O., "Numerical Study of Sound Generation due to a Spinning Vortex Pair," *AIAA Journal*, Vol. 33, No. 1, 1995, pp. 20-26.

[19] Lele, S. K., "Compact Finite Difference Schemes with Spectral-like Resolution," *Journal of Computational Physics*, Vol. 107, 1993, pp. 262-281.

[20] Watson, W. R., and Myers, M. K., "Inflow-Outflow Boundary Conditions for Two-Dimensional Acoustic Waves in Channels with Flow," *AIAA Journal*, Vol. 31, No. 9, 1993, pp. 1574-1582.